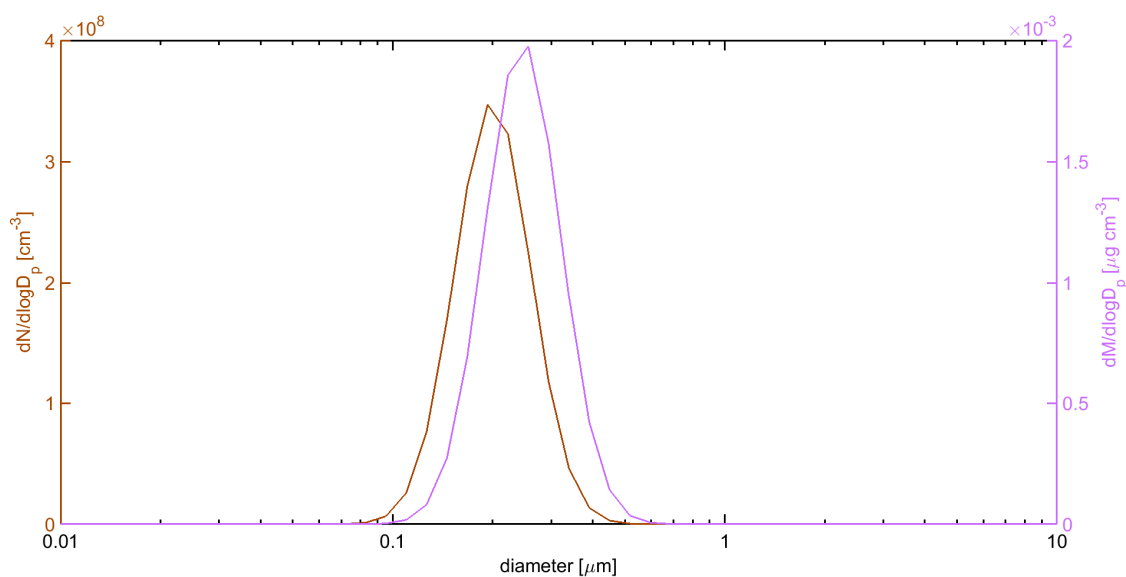


## Supplementary Material

### *Description of the Sensitivity Analysis of The Model*

To test the performance of the model we tested the effect of the input-parameters on the output of the model. The analysis was done using a source emitting lognormally distributed particles having a geometric mean diameter of 200 nm, a standard deviation of 1.3, and source strength of  $1.7 \times 10^{11} \text{ s}^{-1}$  (the number and mass distributions for the source are found in figure S1). The source was active one fourth of the total modelling time. The simulated total volume was of  $40 \text{ m}^3$  ( $2.5 \times 4 \times 4 \text{ m}^3$ ), which was divided to a NF and a FF volume. The NF was considered to be  $2 \times 2 \times 2 \text{ m}^3$  in the centre of the room and the FF to be the remainder of the room volume. The sensitivity analysis was carried out by varying one input-parameter using a one-at-a-time analysis<sup>36</sup> while other parameters were kept constant. Evaluation is based on acute exposure calculated as the 15-minute time weighted average. The following parameters were chosen for the sensitivity test: source strength, ventilation flow rate, density, and friction velocity. The parameters were varied in 5 steps from -50 % to +100 % of an initial chosen value (see table S2). During the sensitivity analysis, the computational time on a standard desktop computer with an i3 Intel CPU and 16 GB RAM was in the order of 1-10 sec.

Results from the sensitivity test with a variation of 0 % of the input parameters are shown in figure S3. S3A shows the total number concentration. S3B shows that the cumulated mass and shows that the amount of mass that enters the chamber (In) is equal to the mass that is inside the chamber (Remaining) plus the losses in chamber through deposition and ventilation (Out). The size distributions shown in S3C and S3D shows that there is coagulation and size dependant deposition occurring in the chamber. Figure S4 shows the change 15-minutes time weighted average concentrations for both number (S4A) and mass (S4B) in both near field and far field as a function of the variation of input parameters. It show a strong dependence of source strength with increasing concentrations in both near field and far field with increased mass introduced into the chamber. With the flow rate decreases concentrations in the near field while increasing concentrations in the far field due to faster transport between near field and far field. The opposite is seen for lower flow rates  $Q$ . change in friction velocity affects only minor the concentrations. For number concentrations the density has minor influence while for the mass concentrations the effect is similar to an increase in the source strength.



**Figure S1.** number and mass distribution for the constant source used in the sensitivity analysis.

**Table S2.** Parameters and variations for the one at a time sensitivity analysis of the model

Variation	-50%	-25%	0%	+50%	+100%
Source strength multiplied by	0.5	0.75	1	1.5	2
Ventilation flow rate, $Q$ [ $\text{m}^3 \text{s}^{-1}$ ]	0.011	0.017	0.022	0.033	0.044
Density [ $\text{g cm}^{-3}$ ]	0.5	0.75	1	1.5	2.0
Friction velocity [ $\text{cm s}^{-1}$ ]	0.005	0.075	0.01	0.015	0.02

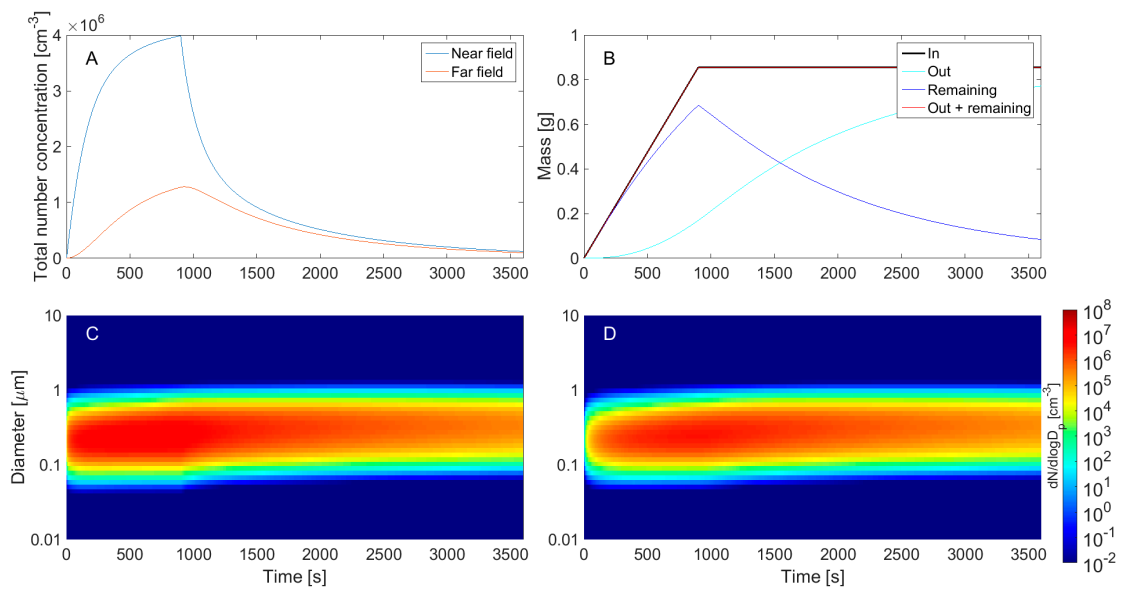


**Figure S3.** concentrations and mass balance of the sensitivity analysis run for 0% variation of input parameters. **(A)** The total number concentration in the far field and near field. **(B)** Cumulative mass balance. **(C)** and **(D)** particle size distributions in near field and far field, respectively.

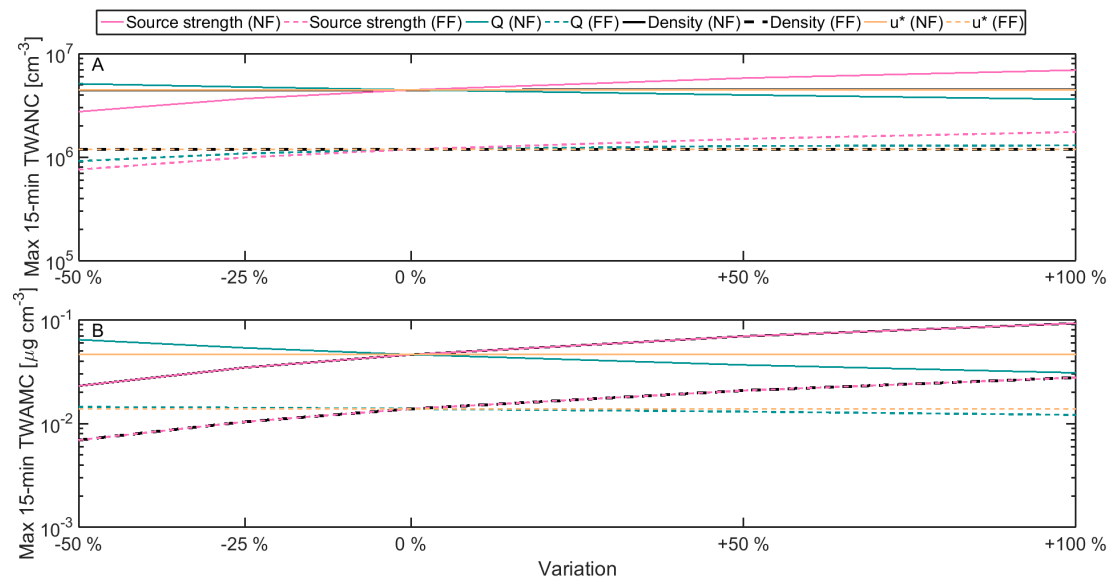


**Figure S4.** 15-minutes time weighted averages of near field (NF) and far field (FF) concentrations for sensitivity analysis of the following parameters: Source strength, density, friction velocity ( $u^*$ ), and ventilation flow rate,  $Q$ . The maximum 15-minutes time weighted average number concentration (TWANC) and the maximum 15-minutes time weighted average mass concentration (TWAMC) are shown in A and B, respectively.

Table S5: Description of aerosol instruments used in the experiment.

Instrument	Location	Model Type	Measured properties
Scanning mobility particle sizer (SMPS)	Source	3081, 3082, 3088, TSI Inc., Shoreview, MN, USA	Optical number concentration and electrical mobility size distribution in 100 size channels with a 1 min resolution
Condensation particle sizer (CPC)	Near field Far field 1 <sup>†</sup> ,2 <sup>†</sup> ,*3,4	3007, TSI Inc., Shoreview, MN, USA	Optical number concentration, 10 nm to >1 $\mu\text{m}$ with a 1 hz resolution
Fast mobility particle sizer (FMPS)	Near field Far field 2,4	3091, TSI Inc., Shoreview, MN, USA	Electrical mobility number concentration and size distribution in 32 size channels ranging from 5.6 nm to 560 nm with a 1 hz resolution

<sup>†</sup>only for experiment E2 and E3; \*only for experiment E1 and E2

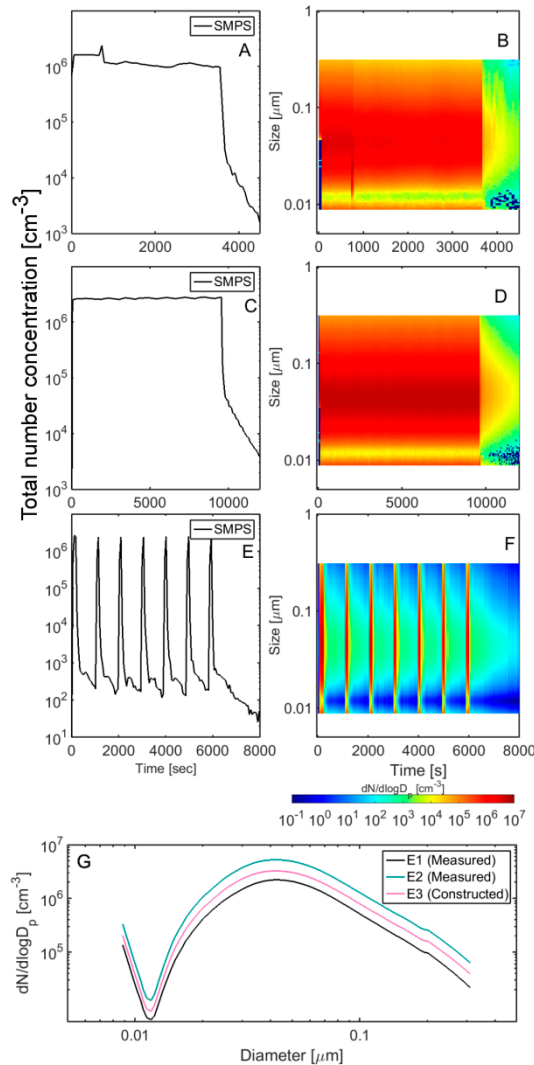


**Figure S6.** shows the total number concentrations and particle size distribution measured by the SMPS near the source during E1 (A, B), E2 (C, D), and the constructed source for E3 (E, F). G show the mean size distribution for the time when the source is active.

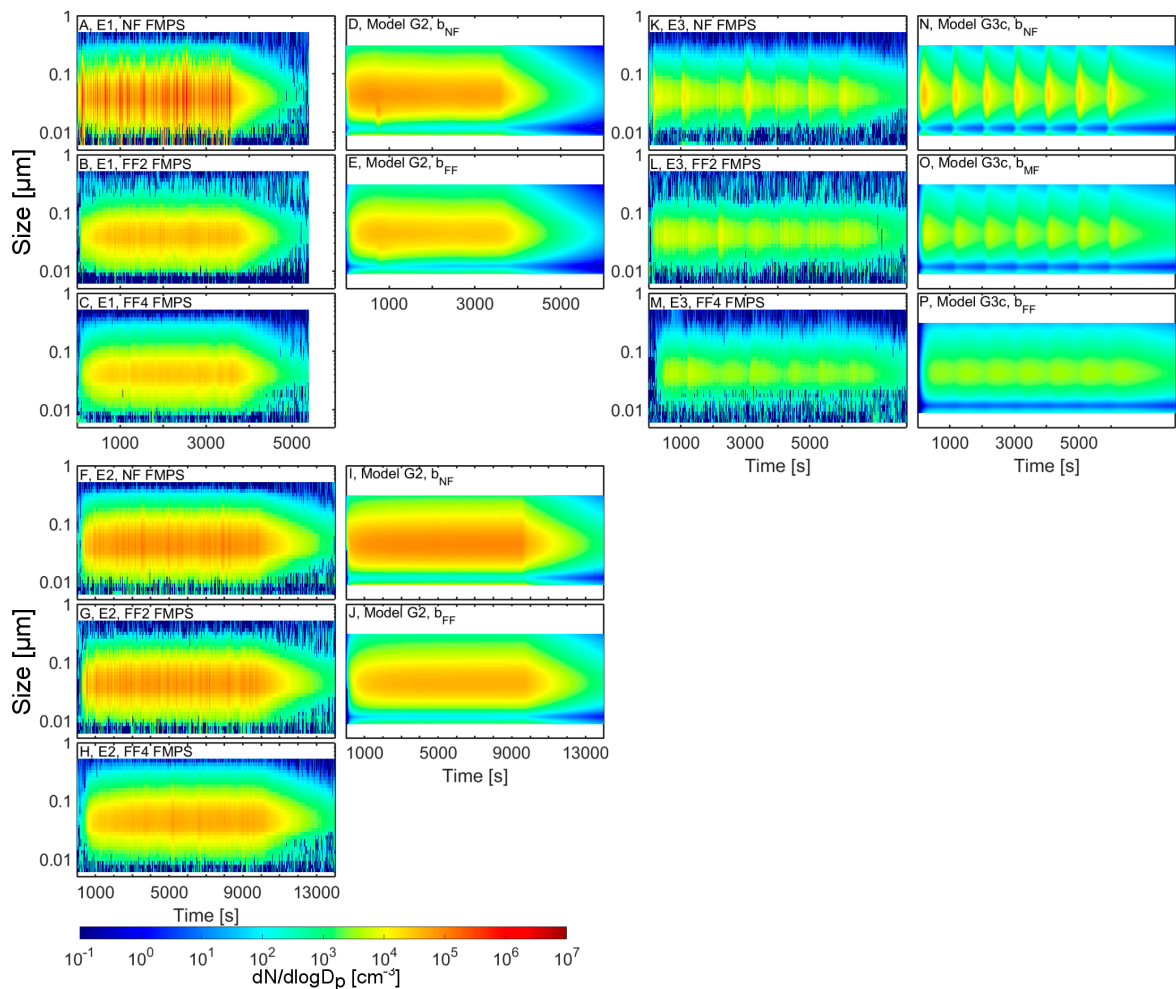


**Figure S7.** measured size distributions by the FMPS in NF, FF2 and FF4 positions and the modelled concentrations using the layout that provided the best fit. For E1 the measured FMPS concentrations are shown in **A**, **B**, and **C** for the NF, FF2, and FF4 positions, respectively, and compared with the modelled G2 layout is shown in **D** and **E** for  $b_{NF}$  and  $b_{FF}$ , respectively. For E2 the measured FMPS concentrations are shown in **F**, **G**, and **H** for the NF, FF2, and FF4 positions, respectively, and compared with the modelled G2 layout is shown in **I** and **J** for  $b_{NF}$  and  $b_{FF}$ , respectively. For E3 the measured FMPS concentrations are shown in **K**, **L**, and **M** for the NF, FF2, and FF4 positions, respectively, and compared with the modelled G3c layout is shown in **N**, **O**, and **P** for  $b_{NF}$ ,  $b_{MF}$ , and  $b_{FF}$ , respectively.

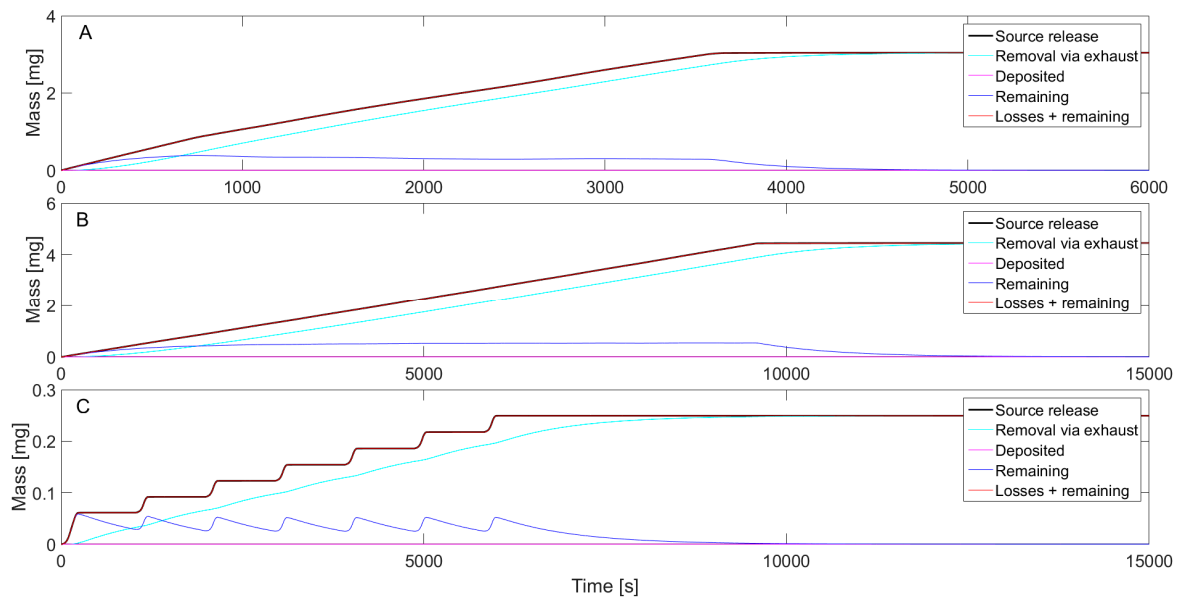


**Figure S8.** Cumulative mass balance for E1 (A), E2 (B), and E3 (C) using the two-box layout.

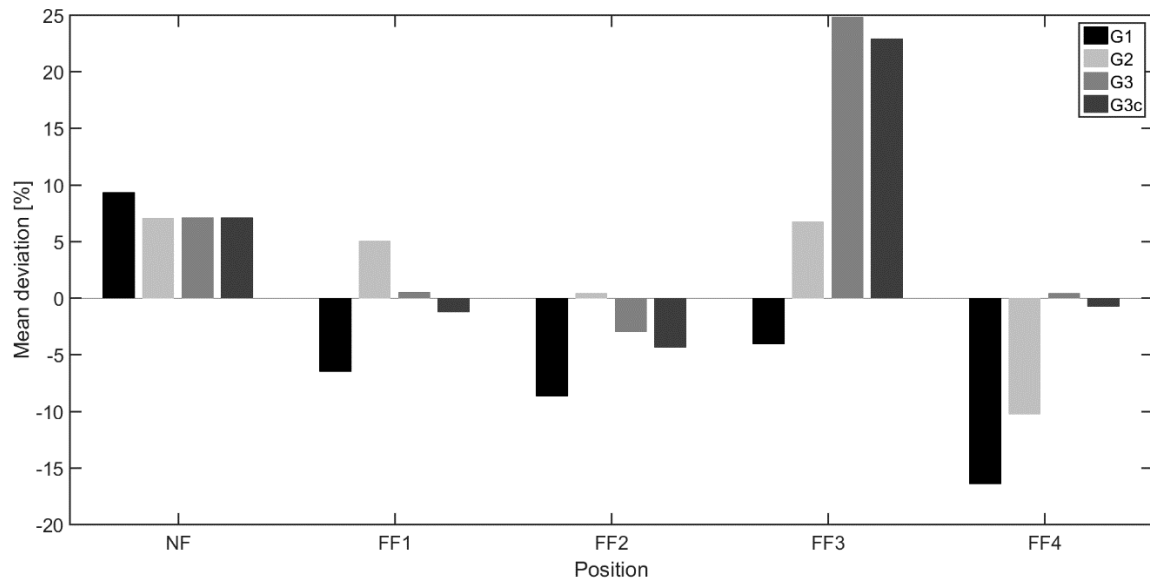


**Figure S9.** Statistical analysis on the timing of peak concentrations in the measurement positions for the four considered geometrical layouts. Negative values mean, that the peak precedes in the model.